

Plasma Wind Tunnel Test Design Methodologies for Re-entry Vehicle Components

S. Di Benedetto, M. Di Clemente and M. Marini

*CIRA, Italian Aerospace Research Centre
81043 Capua, Italy*

Abstract

Hypersonic flows are characterized by high speed and high energy content. These features make extremely difficult the design of ground-based experiments (extrapolation from flight procedure), since the full duplication in ground facilities of flow characteristic numbers (Mach, Reynolds) and state of the gas (Damkhöler) is not feasible. On the other side, ground facility testing is one of the main simulation tools used in the design of a re-entry vehicle and is needed to qualify re-entry vehicle components in a relevant plasma environment. A test design methodology has been developed in order to perform test campaigns in the CIRA Plasma Wind Tunnel “Scirocco”. Starting from the phenomena we want to reproduce on a test model, the test requirements, a theoretical-numerical procedure has been carried out in order to properly define the facility set-up (nozzle configuration, total pressure and enthalpy inside the test chamber, model position) able to match the test requirements, preliminary defined by means of CFD simulations in critical flight conditions. The developed methodology is explained in details in this paper, and some applications on typical re-entry vehicle components are shown as well.

1. Introduction

One of the most challenging problems of modern aerospace engineering is the prediction of high speed flows characterised by very complex physical phenomena. Difficulties are due to: the high energy content of these flows, that makes extremely difficult the design of ground-based experiments; the complexity of the physical phenomena that have to be predicted by CFD simulations; the lacking of flight data.

On the other hand ground facility simulations, numerical methods and in-flight simulations are the suitable simulation means that have to be combined and mutually validated, both to improve understanding of high-speed high-energy flows for research activities and to make possible the design of a hypersonic vehicle.

To underline the necessity of this tools combination, often the term “simulation means triangle”^[1] is adopted and is schematically represented in the following Figure 1:

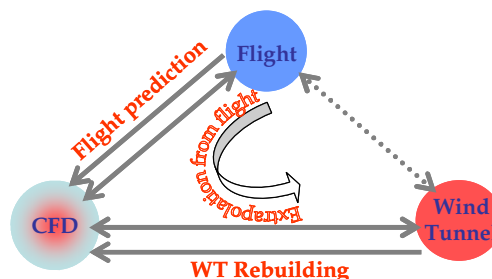


Figure 1: Simulation means triangle

The dotted line, that links ground and in flight testing, highlights the impossibility of contemporarily reproducing in a wind tunnel all the flight parameters: Mach number, Reynolds number, chemical state of the gas, energy distribution, model dimension. For hypersonic flight, one of the most important features to model is the heat flux transferred to the surface, but, since ground facilities, as said above, are far from reproducing the real operating conditions of a

hypersonic re-entry vehicle, CFD has to be used to understand test conditions necessary to reproduce on a representative model the same values of heat flux and pressure loads that vehicles experience during the re-entry trajectory, being the aim to test Thermal Protection System, TPS, materials of such vehicles.

The design of ground-based experiments based on theoretical-numerical analysis of simulated flight conditions is called *extrapolation from flight*.

An extrapolation from flight methodology has been developed in order to perform test campaigns in the CIRA Plasma Wind Tunnel “Scirocco” and will be described in details in section 3. Then three different applications of the methodology will be described. For all the tests presented, a flight experiment is foreseen, in order to make possible the *extrapolation to flight* and, therefore, the triangle’s accomplishment.

2. Facility description

The CIRA Plasma Wind Tunnel “Scirocco” is devoted to aerothermodynamic tests on components of aerospace vehicles; its primary mission is to simulate (in full scale) the thermo-fluid-dynamic conditions suffered by the Thermal Protection System (TPS) of space vehicles re-entering the Earth atmosphere.

“Scirocco” is a very large size facility, whose hypersonic jet impacts the test article having a diameter size up to 2 m and reaches Mach number values up to 11. The jet is then collected by a long diffuser (50 m) and cooled by an heat exchanger. Seventy MW electrical power is used to heat the compressed air that expands along a convergent-divergent conical nozzle. Four different nozzle exit diameters are available: 0.9, 1.15, 1.35 and 1.95 m, respectively named C, D, E and F.

The overall performance of “Scirocco” in terms of reservoir conditions is the following: total pressure (P_0) varies from 1 to 17 bar and total enthalpy (H_0) varies from 2.5 to 45 MJ/kg. Lower enthalpy values are obtained by using a plenum chamber between the arc heater column exit and the nozzle inlet convergent part, which allows transverse injection of high pressure ambient air to reduce the flow total enthalpy.

The energetic heart of the facility is the segmented constricted arc heater, a column with a maximum length of 5.5 m and a bore diameter of 0.11 m. At the extremities of this column there are the cathode and the anode between which the electrical arc is generated. A power supply feeds the electrical DC power to the electrodes for the discharge. A compressed air supply distributes dry compressed air to the various segments of the arc heater column, being able to supply a mass flow rate ranging from 0.1 to 3.5 kg/s, heated up to 10000 K.

The last important subsystem of “Scirocco” is the vacuum system, which generates the vacuum conditions in test chamber required by each test. The system consists of ejectors that make use of high pressure water steam as motor fluid (30 bar and 250 °C).

Facility theoretical performance map in terms of reservoir conditions produced by the arc heater is shown in Figure 2.

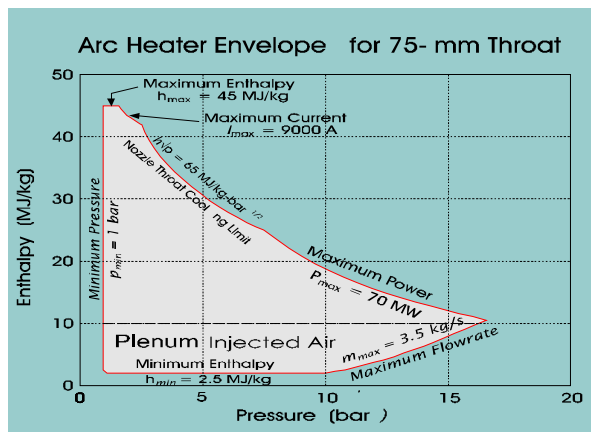


Figure 2: Arc heater theoretical performance map

The achievement of the operating conditions (P_0 , H_0) in test chamber is assured by the presence, before the insertion of the model, of a 100mm-diameter hemi-spherical calibration probe made of copper, cooled, that measures radial profiles of stagnation pressure (P_s) and stagnation heat flux (Q_s) at a section 0.375 m downstream of the conical nozzle exit section, by means of high precision pressure transducers and Gardon-Gage heat flux sensors, respectively. Facility regulations (mass flow, current) are tuned in order to measure on the calibration probe a certain couple of values (P_s , Q_s) which correspond to the desired set point in terms of the couple (P_0 , H_0).

3. Test design methodology

The extrapolation from flight procedure is complicated by the circumstance that many differences exist between flight and PWT conditions (model dimension, dissociated inlet conditions in test chamber, density level, etc.). These aspects play an important role on the non-equilibrium phenomena and make difficult the extrapolation of real flight to wind tunnel conditions. The main problem is to find the correct similitude parameters and to do this, we firstly need to define the goal of the simulation, that is the phenomenon we want to reproduce; this is often a flight condition to be simulated in wind tunnel (extrapolation from flight, see section 1), but it can be a particular customer's request as well.

Firstly, a test feasibility verifies the compatibility of requirements with the PWT theoretical envelope and of test article dimensions with test chamber capability, in order to avoid blockage phenomenon. Then, a first operating condition is defined by means of both engineering tools, to derive the stagnation point heat flux and pressure from requirements on the test article, and the curve-fit calibration law DART for fast PWT Test Setting^[2]. This latter links the driving parameters of the facility (current and air mass flow) and the PWT performances in terms of reservoir pressure (P_0) and reservoir enthalpy (H_0), and consequently to stagnation pressure (P_s) and stagnation heat flux (Q_s) on the PWT calibration probe.

Starting from the preliminary condition, the final PWT condition able to match the test requirements has been defined by means of an iterative procedure, which involves both two dimensional CFD computations and evaluations with simplified engineering correlations and which is schematically described in Figure 3. Test chamber conditions to be used for the simulation of the flow around the model in test chamber are obtained from the numerical computation of the nozzle flow. If the CFD simulation of the flow past the model shows that test requirements over the model are not still achieved, a new reservoir condition (P_0 , H_0) is deduced by using simplified engineering correlations and the procedure restarts from the CFD simulation of the nozzle flow. As an alternative, test requirement fulfilment could be reached with the same reservoir condition, opportunely modifying the model position inside the test chamber and/or the model attitude. In this last hypothesis only model computation has to be iterated.

Once the final PWT operating condition has been defined, numerical computation on the PWT calibration probe provides pressure (P_s) and heat flux (Q_s) at the probe stagnation point. These values, measured during the test, ensure the achievement of the desired operating condition in terms of (P_0 , H_0) in test chamber.

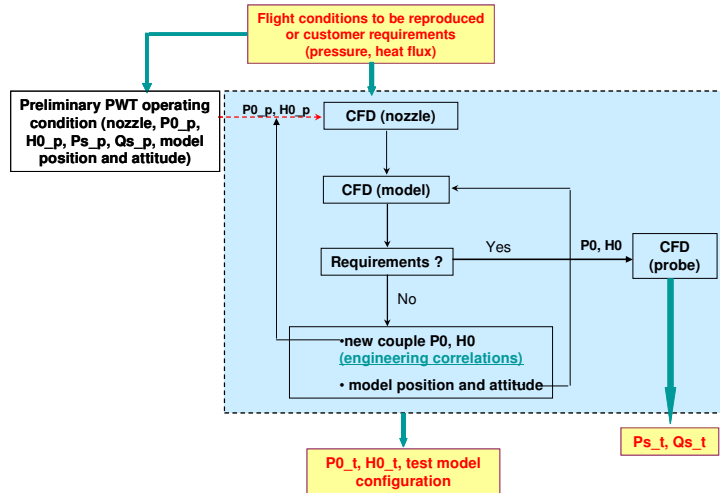


Figure 3: Test design iterative procedure

Engineering correlations used in the above procedure are generally derived from isentropic relations for stagnation pressure, and from the Fay-Riddell semi-empirical correlations for stagnation heat flux^[3]:

$$p_{0,T} = \frac{p_0}{p_{st}} p_{st,T} \quad (1)$$

$$H_{0,T} = \frac{\dot{Q}_{st,T}}{\sqrt{\frac{p_{st,T}}{p_{st}}}} (H_0 - c_p T_{st}) + c_p T_{st,T} \quad (2)$$

where the subscript T distinguishes the “Target” values (i.e. the test requirements) from the current ones and indicates the new PWT test condition in terms of total enthalpy and total pressure. $Q_{st,T}$ and $P_{st,T}$ constitute the heat flux and pressure at the model stagnation point needed to ensure the test requirements.

The above explained test design methodology was successfully applied in recent past for IRT capsule PWT testing activities^[4], a program funded by ESA and led by the Italian company AERO SEKUR.

4. Numerical tool

CIRA code H3NS has been used to perform two-dimensional and three-dimensional computations. It is a structured multiblock finite volume solver that allows for the treatment of a wide range of compressible fluid dynamic problems.

The fluid is treated as a mixture of perfect gases in the case of thermo-chemical non equilibrium flows. The chemical model for air is due to Park and it is characterized by 17 reactions between the five species (O, N, NO, O₂, N₂), neglecting the presence of inert gas in the air (e.g. Ar). The energy exchange between vibrational and translational modes is modelled with the classical Landau-Teller non-equilibrium equation, with average relaxation times taken from the Millikan-White theory modified by Park. For what concerns transport coefficients, the viscosity of the single species is evaluated by a fit of collision integrals calculated by Yun and Mason, the thermal conductivity is calculated by means of the Eucken law; the viscosity and thermal conductivity of the gas mixture are then calculated by using the semi-empirical Wilke formulas. The diffusion of the multi-component gas is computed through a sum rule of the binary diffusivities of each couple of species (from the tabulated collision integrals of Yun and Mason). Transport coefficients, in the hypothesis of an ideal gas, are derived from Sutherland’s law, suitably modified to take into account low temperature conditions.

With respect to the numerical formulation, conservation equations, in integral form, are discretised by means of a finite volume, cell centred, technique. Eulerian fluxes are computed with a Flux Difference Splitting method, and second order formulation is obtained by using a ENO-like reconstruction of interface values. Viscous fluxes are computed with a classical centred scheme. Time integration is performed by employing an explicit multistage Runge-Kutta algorithm coupled with an implicit evaluation of the chemical and vibrational source terms.

5. Applications

In this section, applications of the above explained test design procedure relatively to the plasma tests of typical re-entry vehicle components will be shown. In particular, the procedures followed in three test design activities on going at CIRA will be detailed. The first application pertains to a TPS tile (built with both Ultra High Temperature Composite, UHTC, ZrBr₂ and C-SiC) that will be mounted on the future CIRA re-entry vehicle USV-X nose-fuselage junction, and for which one point of the re-entry trajectory (i.e. the point of maximum heat flux) in terms of heat flux and pressure has to be reproduced on a mock-up. The other two applications deal with the tests which will be performed on two components of the EXPERT capsule^[5]: i) the full-scale deflected ceramic flap (the goal being to subject the flap qualification model to the maximum heat flux compatible with the facility performance, to qualify the flight sensing equipment and to observe the physical phenomena which happen inside the flap cavity with an Infra-Red, IR, camera), and ii) the UHTC winglet (the goal being to reproduce on the winglet qualification model the total thermal load which it will be subjected to during the EXPERT re-entry trajectory).

5.1 TPS tile

This test is devoted to the study of innovative materials to be used as Thermal Protection Systems for re-entry vehicles and is linked with a flight passenger experiment designed for the future CIRA re-entry vehicle USV-X.

The flight experiment foresees two TPS tiles (called Bread-Boards, B/Bs), mounted side by side, and built with both UHTC and C-SiC, on the USV-X nose-fuselage junction, in order to subject the two different materials to the maximum heat flux encountered during flight.

For the “Scirocco” test, two Bread-Boards have been designed (one in UHTC ZrBr₂, the other in C-SiC), the goal being to reproduce in PWT the same thermal and mechanical loads of the flight. Consequently, they have been designed regarding the thermal loads on the USV-X 1100_NG re-entry trajectory and referring to the USV-X nose geometry^[6]. The latter can be well approximated by a sphere-cone geometry with a 100 mm radius and axis at an angle of 7.5 deg with respect to the longitudinal body axis, as shown in Figure 4 where the TPS tiles position is also indicated.

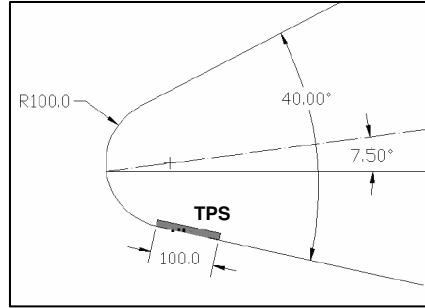


Figure 4: USV-X nose geometry and B/B position (dimensions in mm)

The inputs for the Test Design procedure (see Figure 3) are the flight conditions to be reproduced, that in this case correspond to heat flux and pressure values predicted on the B/Bs in the USV FTB-X trajectory point of maximum heat flux (Mach 19.2; altitude 68.9 km; AoA=25.17 deg). CFD computations performed on the three-dimensional geometry return as heat flux and pressure mean values on the TPS tiles; respectively, 350 kW/m² and 750 Pa. Therefore, these values have to be reproduced on the B/Bs surface in the “Scirocco” test.

The tile model realized for the test is shown in Figure 5, in the case of UHTC B/B; the same concept has been adopted for the C-SiC one. During the test the B/Bs will be mounted on the PWT calibration probe support, whose diameter is 100 mm. Distance from nozzle exit to calibration probe stagnation point is 37.5 cm.

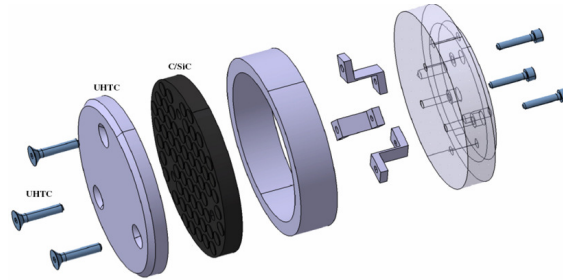


Figure 5: UHTC B/B concept

In Table 1 is reported the PWT preliminary operating condition, deduced by fit-law based engineering tools^[2].

Table 1: PWT preliminary operating conditions

| Nozzle configuration | F |
|-------------------------------------|--|
| | exit diameter=1.95 m length from the throat section=5.370 m |
| Total pressure P ₀ | 2.2 bar |
| Total enthalpy H ₀ | 17.4 MJ/kg |
| Stagnation Pressure P _S | 7.0 mbar |
| Stagnation Heat Flux Q _S | 760 kW/m ² |

The stagnation pressure P_S and heat flux Q_S are those predicted on the PWT hemi-spherical 100 mm diameter calibration probe by properly scaling the model requirements.

Since the B/B length has not been still frozen, a parametric analysis has been conducted, considering four possible lengths (5 cm, 10 cm, 15 cm, 20 cm), measured starting from the PWT calibration probe section (42.5 cm downstream the nozzle exit), once the hemispherical copper cap has been taken away.

The formula adopted for the stagnation point heat flux is a particular expression of the Fay-Riddell correlation, where the constants have been obtained by means of PWT experimental results fits:

$$Q_s = 100 \cdot \sqrt{\frac{P_s}{R}} \left[172.8 \cdot (H_{0,T} - c_p T_s) - 270.5 \right] \quad (3)$$

Result in terms of total enthalpy has then been corrected by considering that flat faced model heating is equivalent to that realized on a sphere of effective nose radius (R_{eff}) equal to $2.9R_b$, being $R_b=50$ mm the base radius of the body^[7]. The final PWT test condition, produced by the present test design methodology, is then defined in Table 2, together with the CFD results both for the calibration probe stagnation point and for the test article.

Table 2: Final PWT test condition (P_s, Q_s) and CFD results ($P_{B/B}, Q_{B/B}$)

| Nozzle F, $P_0=2.4$ bar, $H_0=14.7$ MJ/kg | |
|---|-----------------------|
| P_s | 717 Pa |
| Q_s | 834 kW/m ² |
| $P_{B/B}$ | 730 Pa |
| $Q_{B/B}$ | 357 kW/m ² |

Hereinafter, in Figure 6, Mach number contours are shown, while heat flux and pressure distributions on the B/B centerline obtained with the final PWT condition are reported in Figure 7. The following effects have been evaluated: B/B length, curvature model radius, wall catalycity.

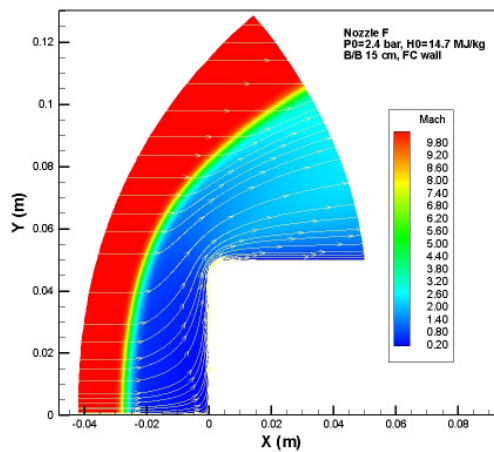


Figure 6: Mach number contours and streamlines

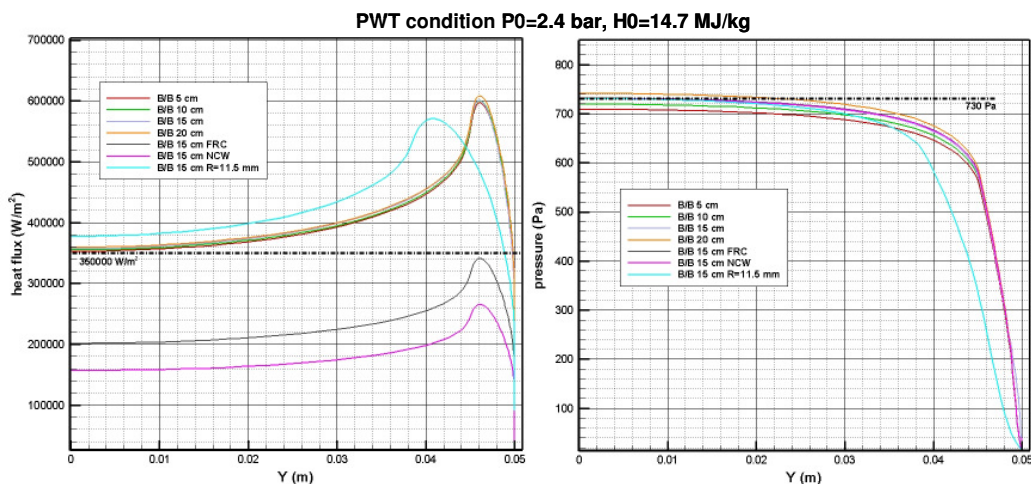


Figure 7: Heat flux (left) and pressure (right) distributions on the B/B surface

The B/B length effect can be considered negligible on all B/B surface properties with respect to the goal of the experiment. Analysis of curvature radius and catalycity effects has been conducted just for one B/B length (15 cm).

Heat flux predicted in the non catalytic wall hypothesis is more than one half lower with respect to the fully catalytic one. The effect of a curvature radius increase is a slight raise of heat flux on the B/B middle part and a decrease of heat flux peak on the shoulder, as expected.

It can be concluded that present test design methodology has produced a test condition that properly fulfils test requirements both in terms of heat flux (+ 2%) and pressure (- 2.6%).

5.2 EXPERT full scale flap

The main objective of this test is to experimentally investigate the thermo-mechanical behaviour of the EXPERT vehicle full-scale flap^[5] in the “Scirocco” Plasma Wind Tunnel, realizing one test model configuration with the same cavity of the actual flap, built using the same materials (C-SiC for the flap and PM1000 for the cavity) and equipped with a reduced set of the in-flight flap instrumentation and with the full IR thermocamera assembly and interfaces of the in-flight cavity, so to include in the test the plasma qualification of the EXPERT flap-cavity sensing equipment. From three-dimensional computations^[8] it comes out that, in the EXPERT 5 km/s trajectory point of maximum heat flux (i.e. $M=13.99$), the flap is subjected to a very high heat flux; values varies from 800 kW/m^2 , in the hypothesis of fully turbulent flow, to 1300 kW/m^2 in the more critical situation of laminar-to-turbulent transition at reattachment point on the flap. Such high values, as it has been verified by means of CFD simulations, are not reproducible in PWT, so the goal of this test is to reproduce the maximum heat flux compatible with both the geometry of the EXPERT actual flap and the “Scirocco” facility performance. In this way the flap will be just partially qualified. The focal point of the test will be the study of the physical phenomena which occur inside the flap cavity, detached by the IR thermocamera; in particular, to have information about the vortex reattachment heating inside the cavity and the radiative heat exchange between the surface of the cavity and the back face of the flap.

Views of the actual EXPERT flap and of the test article (flap and cavity) for the PWT test are reported in Figure 8.

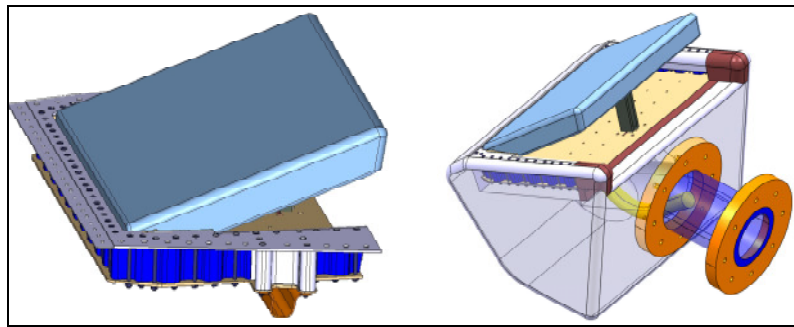


Figure 8: EXPERT actual flap (left) and flap test article (right)

At the time of test design execution the test article geometry was not still frozen. For this reason test design methodology has been applied for two possible configurations: a) holder nose curvature radius 3.75 mm, flap deflection 55 deg; b) holder nose curvature radius 3.50 mm, flap deflection 45 deg. Predicted temperature contours on the symmetry planes, where computations have been performed, are shown in Figure 9.

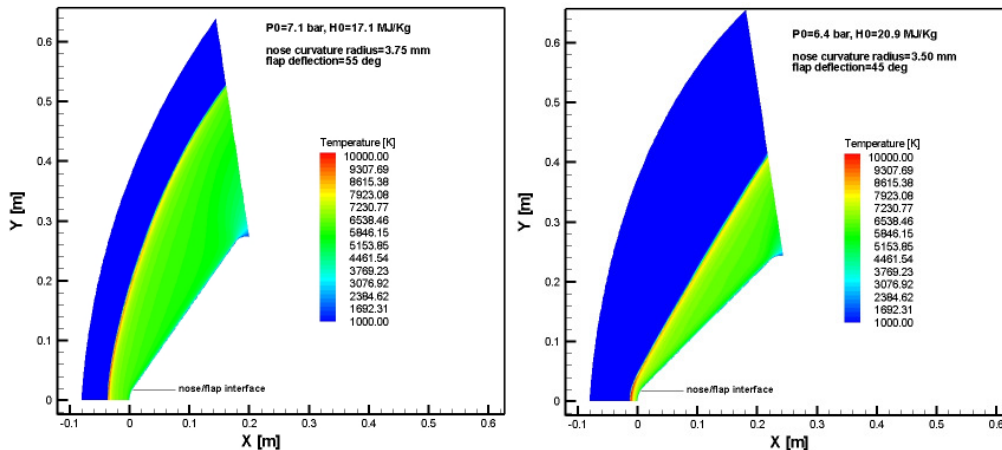


Figure 9: Temperature contours: case a), left; case b), right

Total enthalpy and total pressure values reported in figure are relative to the final PWT operating conditions deduced by adapting the general test design methodology to the current case, and by using the following reasoning.

Initially a requirement of 1300 kW/m^2 at the nose/flap interface, NFI, has been supposed ($\dot{Q}_{NFI,T}=1300 \text{ kW/m}^2$), to which corresponds, in the hypothesis of radiative equilibrium, a requirement in terms of surface temperature: $T_{NFI,T}=(\dot{Q}_{NFI,T}/\sigma\varepsilon)^{1/4}$.

Heat flux at the nose/flap interface can be expressed by means of Fay-Riddell concepts for stagnation point heat flux and Beckwith-Gallagher correlation for the heat flux distribution around a circular cylinder of radius R ^[3]:

$$(\dot{Q})_{NFI} \cong \sqrt{\frac{P_s}{R}} (H_0 - c_p T_s) (a \cos^{3/2}(\theta_{NFI}) + b) \quad (4)$$

where θ_{NFI} is 35° deg in case a) and 45° deg in case b). From equation (4) heat flux and temperature required at the stagnation point can be deduced:

$$(\dot{Q})_s = \frac{(\dot{Q})_{NFI}}{a \cos^{3/2}(\theta_{NFI}) + b} \Rightarrow T_s = \left(\frac{(\dot{Q})_s}{\varepsilon\sigma} \right)^{1/4} \quad (5)$$

and then $Q_{S,T}$ and $T_{S,T}$ as well.

Then, once having defined and simulated the preliminary test condition, the new test condition in terms of $H_{0,T}$ able to realize $Q_{NFI,T}$, supposing the same value of P_0 (P_s), is:

$$H_{0,T} \cong c_p T_{s,T} + \frac{(\dot{Q})_{NFI,T}}{(\dot{Q})_{NFI}} (H_0 - c_p T_s) \quad (6)$$

where Q_{NFI} and T_s have been provided by CFD simulation of flow past the flap model.

Comparison of in-flight heat flux distributions^[8] with that obtained in PWT conditions (see Figure 10) shows the impossibility of reproducing the mean heat flux value on the flap, as it was expected. Lower heat flux values achieved with 55 deg flap deflection are due to the greater entropy layer that develops in this case, as it is clear from the shock wave curved shape in Figure 9. In fact, entropy layer development causes a deterioration of model surface properties; for example, wall pressure is no more constant along the flap surface.

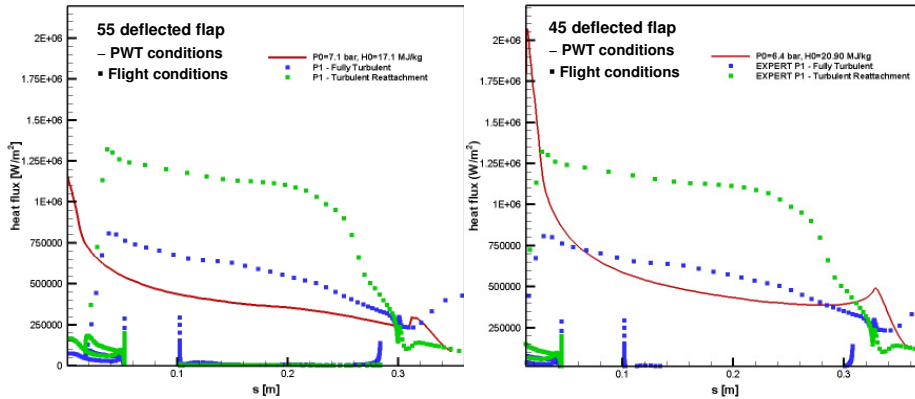


Figure 10: PWT and in-flight heat flux distribution comparisons: case a), left; case b), right

The final PWT condition, with the flap test model inclined by 45 deg and nose radius of curvature or 3.5 mm, is then reported in Table 3, also with the results predicted at the calibration probe stagnation point and the heat flux and temperature predicted at the nose/flap interface.

Table 3: Final PWT test condition (P_s , Q_s) and CFD results (Q_{NFI} , T_{NFI})

| Nozzle D, $P_0=6.4$ bar, $H_0=20.9$ MJ/kg | |
|---|-----------------------|
| P_s | 4540 Pa |
| Q_s | 3030 kW/m^2 |
| Q_{NFI} | 1207 kW/m^2 |
| T_{NFI} | 2271 K |

5.3 EXPERT winglet

This test is dedicated to the EXPERT scientific Payload#15^[5], developed by CIRA, consisting of two massive UHTC $ZrBr_2$ winglets placed on the capsule surface in diametrically opposite positions. Test aim is to reproduce, on a winglet qualification model, the total thermal load and, if it is realizable, the maximum temperature which the winglet is subjected to during the 5 km/s EXPERT re-entry trajectory, in a relevant plasma environment. During the test, the winglet qualification model will be mounted on a properly designed model holder (see Figure 12) and will be instrumented with four pressure taps and two thermocouples.

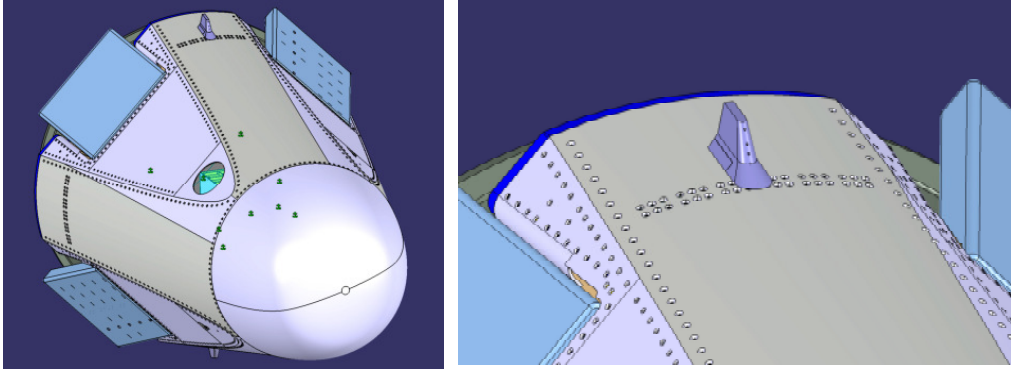


Figure 11: Winglet mounted on the EXPERT capsule

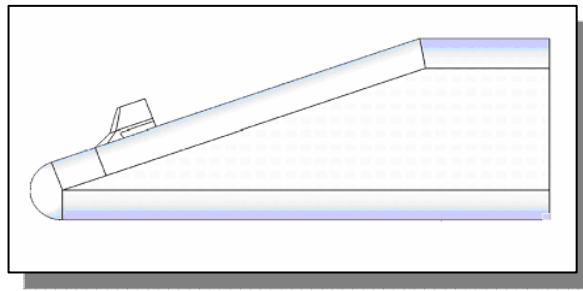


Figure 12: Winglet mounted on the PWT model holder

This test design procedure differs from the formers for two fundamental reasons:

- due to the high temperatures predicted in flight conditions and to the circumstance that test aim is mainly the total thermal load reproduction, PWT operating condition is defined as the one which corresponds to the maximum heat flux measurable on the PWT calibration probe stagnation point (i.e. 3000 kW/m^2);
- due to the impossibility of performing two-dimensional simulations on the complete test article (holder and winglet) centreline, a different solution has been found.

Hence, once having defined a preliminary PWT condition and a possible model holder configuration, looking at the left branch of the flow chart in Figure 3, computations on the test model have been substituted by axi-symmetric simulations realized on the PWT calibration probe, and the adopted correlations have been Eq. (1) and Eq. (2). Then, with the deduced PWT condition, two-dimensional simulations have been performed on the model holder without the winglet.

The scope has been to compare distributions of significant flow variables extracted at various holder streamwise sections (i.e. different possible winglet positions) with analogue features obtained in flight conditions. These latter ones have been drawn by performing two dimensional simulations on the EXPERT capsule symmetry plane and then extracting the section in correspondence of the winglet position.

Holder sections have been extracted both on the flat and on the deflected surface; the comparison between PWT conditions (with different winglet positions) and in-flight condition is shown in Figure 13, finding out that Mach number around the winglet can be well reproduced while pressure obtained in PWT is from 3 until 10 times lower, as it was expected. The best winglet position is the one on the 20 deg deflected plate at $x=0.1 \text{ m}$ from the holder leading edge (the cyan line in Figure 13), since it allows the highest pressure (and temperature) values obtainable avoiding the impingement of the bow shock wave on the winglet.

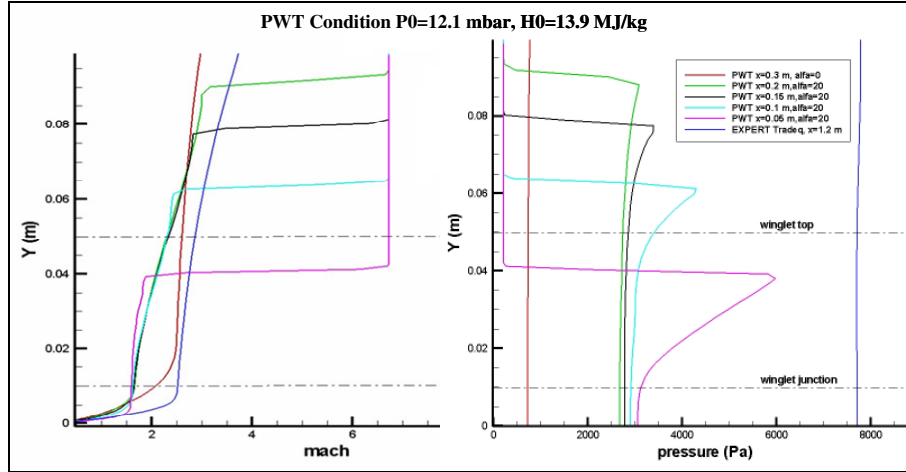


Figure 13: PWT and in-flight Mach number (left) and pressure (right) distributions; effect of different holder sections

In order to evaluate temperature requirement fulfilment and run duration needed to reproduce on the winglet the in-flight thermal load (by using the energy equivalence principle), conditions at the selected holder section have been used as free-stream conditions for a two-dimensional computation on the winglet top profile (on the horizontal plane). The same has been made for the winglet in flight conditions, in such a way to allow meaningful comparisons. Predicted results on the winglet top profile, in the hypothesis of fully catalytic (FC) and radiative equilibrium wall are shown in Figure 14.

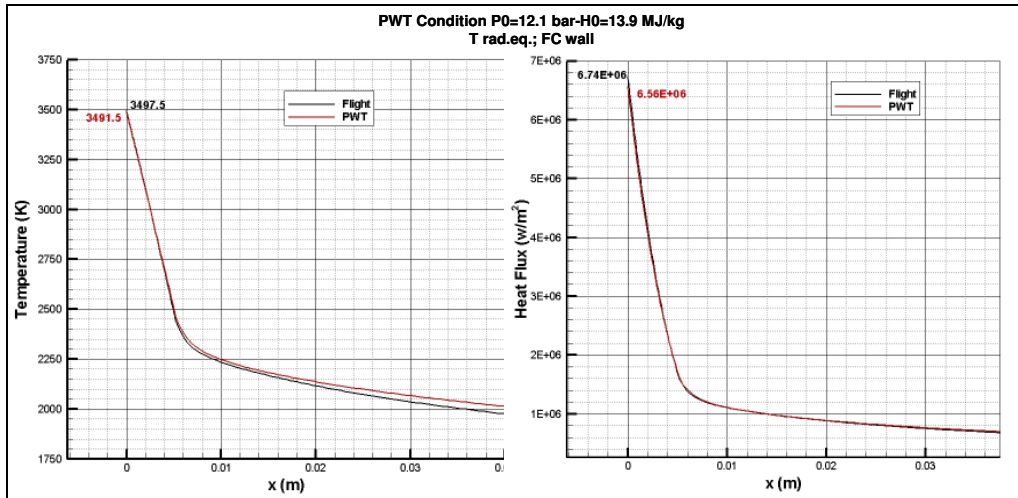


Figure 14: Temperature (left) and heat flux (right) distributions on the winglet top profile in flight and in PWT conditions

Temperature and heat flux values at the stagnation point have then been corrected to take into account that the winglet leading edge is not perpendicular to the flow direction because of the winglet sweep angle^[9], i.e.

$$\dot{Q}_{stag}(\Lambda) = \dot{Q}_{stag}(\Lambda = 0^\circ) \cos \Lambda \quad (7)$$

where Λ is the winglet sweep angle ($\Lambda = \pi/2 - 54.46$ deg) and $\dot{Q}_{stag}(\Lambda = 0^\circ)$ is the stagnation point heat flux value taken from the winglet top slice two-dimensional simulation. Results are summarized in Table 4, where an indication of the reproducibility has been given as the ratio of PWT heat flux to in-flight heat flux. Note that reproducibility is enhanced by considering more realistic surface temperature assumption such as radiative equilibrium.

Table 4: CFD results and reproducibility

| x=0.1 m; α=20 deg | | FC wall | | | |
|-------------------|-------------------|--|-------------------------------|--|-----------------------------------|
| | | Q _{stag} (MW/m ²) Λ=0° | T _{stag} (K) Λ=0° | Q _{stag} (MW/m ²) Λ=35.54° | T _{stag} (K) Λ=35.54° |
| FLIGHT | 300 K | 10,20 | 300,00 | 8,30 | 300,00 |
| FLIGHT | rad.eq. (εps=0.8) | 6,74 | 3491,33 | 5,48 | 3315,94 |
| PWT | 300 K | 8,50 | 300,00 | 6,92 | 300,00 |
| PWT | rad.eq. (εps=0.8) | 6,56 | 3491,50 | 5,34 | 3316,10 |
| | | | | PWT/FLIGHT | 0,83 |
| | | | | PWT/FLIGHT | 0,97 |

As a verification of the goodness of the test design methodology followed for the EXPERT winglet and for the future test rebuilding, three-dimensional CFD simulations on the complete configuration (holder and winglet), in PWT conditions, are actually on going. Some preliminary three-dimensional results are reported in Figure 15.

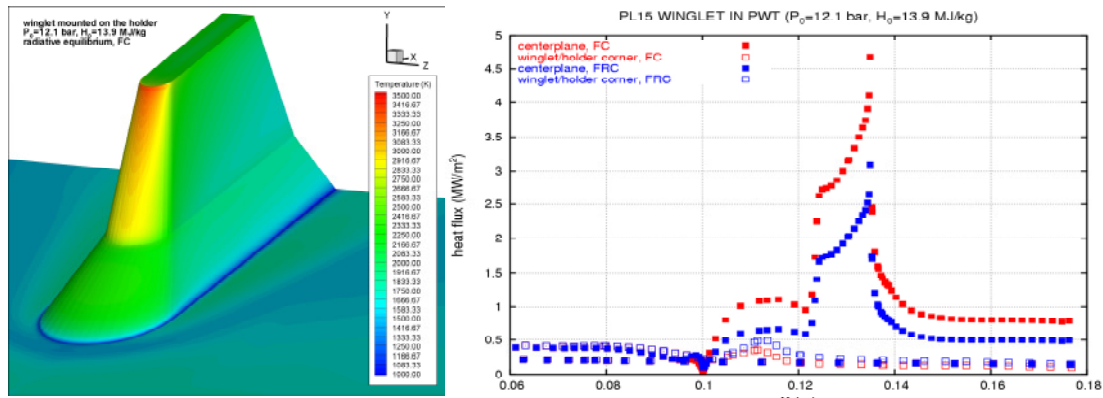


Figure 15: Temperature distribution on the winglet area (left) and heat flux distribution on the winglet's sections (right)

It must be positively evidenced that three-dimensional CFD simulation on the complete model configuration yields a peak heating on the winglet of 4.88 MW/m² with fully catalytic (FC) wall and radiative equilibrium, to be compared to the value of 5.34 MW/m² provided by the test design procedure. Also a more accurate emissivity coefficient (ε=0.66, at the winglet typical operating temperatures) has been used in the full three-dimensional calculations with respect to the one (ε=0.80) preliminarily used in the simplified analysis. The effect of assuming a more realistic catalytic (FRC) behaviour of the UHTC ZrBr₂ material is also clearly evidenced in Figure 15.

The theoretically derived PWT condition is reported in Table 5 together with the results predicted at the calibration probe stagnation point.

Table 5: Final PWT test condition (P_s, Q_s)

| Nozzle C, P ₀ =12.1 bar, H ₀ =13.9 MJ/kg | |
|--|------------------------|
| P _s | 12000 Pa |
| Q _s | 3000 kW/m ² |

Finally, run duration, t_{PWT}, has been evaluated by means of the energy equivalence principle: first, the total energy accumulated by the winglet along the flight trajectory has been calculated and then divided by the heat flux predicted on the winglet in PWT conditions, i.e.:

$$E = \int_{t_i}^{t_f} \dot{q}_{Winglet}^{flight}(t) dt \Rightarrow t_{PWT} = \frac{E}{\dot{q}_{Winglet}^{PWT}} \quad (8)$$

Obviously, in doing that, the bell curve which represents the time history in flight, is approximated by a constant heat flux, therefore the winglet, in PWT, will be submitted to a thermal shock that will not be experienced in flight.

6. Conclusions

This paper has described a Test Design Methodology for aerothermodynamic experiments to be performed in the CIRA “Scirocco” Plasma Wind Tunnel, needed for the design of re-entry vehicle components. The final goal has been the definition of the facility set-up (nozzle configuration, reservoir pressure and reservoir enthalpy inside the test chamber, model position and attitude) able to match the test requirements, preliminarily defined by means of CFD simulations in critical flight conditions on re-entry vehicle’s components, and which involve both evaluations with simplified correlations and accurate CFD computations (extrapolation-from-flight procedure).

In particular, the design procedures followed in three on-going test design activities have been described in detail.

The first application deals with a TPS tile (built with both UHTC $ZrBr_2$ and C-SiC) that will be mounted on the future CIRA re-entry vehicle USV-X nose-fuselage junction, and for which one point of the re-entry trajectory in terms of heat flux and pressure will be reproduced on a mock-up. The second test design activity regards the experiment which will be performed on the EXPERT capsule full-scale deflected C-SiC flap test model, the goal being to reproduce the maximum heat flux compatible with both the geometry of the test article (flap and cavity) and the “Scirocco” facility performance, thus partially qualifying the flap component itself. The last application is dedicated to the test of the EXPERT massive UHTC winglet (Payload#15), whose goal is to reproduce on a winglet qualification model (mounted on a proper holder) the total thermal load and, if possible, the maximum temperature which the winglet will be subjected to during the EXPERT capsule re-entry.

For all these test design activities, feasible “Scirocco” Plasma Wind Tunnel regulations have been selected following the present Test Design Methodology, and the results of simulated PWT conditions have been shown, together with the positive verification of test requirements in terms of model surface properties.

The certified achievement of the test targets on the representative models in a relevant plasma environment (duplication of mechanical and/or thermal loads), obtained through the related experiments scheduled between 2007 and 2008, will demonstrate the reliability the present theoretical-numerical methodology and will finally assure the complete or partial qualification of the re-entry vehicle components.

References

- [1] Hirschel E. H., “Basics of Aerothermodynamics”, Paul Zarchan Editor-in-Chief, Progress in Astronautics and Aeronautics, Volume 204, Springer-Verlag, Berlin, 2005.
- [2] De Filippis F., Caristia S., Del Vecchio A., Purpura C., “The Scirocco PWT Facility Calibration Activities”, 3rd International Symposium Atmospheric Reentry Vehicle and Systems, Arcachon, France, March 2003.
- [3] Anderson J.D. Jr., “Hypersonic and High Temperature Gas Dynamics”, McGraw-Hill Book Company, New York, 1989.
- [4] Marini M., Graps E., “Aerothermodynamic Analysis of a IRT Capsule in Flight Conditions and Design/Execution of Plasma Wind Tunnel Tests”, AIAA paper 2005-3279, May 2005.
- [5] Muylaert J.M. et al., “EXPERT Aerothermodynamic Flight Instrumentation Environment and Integration”, paper IAC-06-D2.6.7, 57th International Astronautical Congress, Valencia, Spain, October 2-6, 2006.
- [6] Schettino A., Pezzella G., Gigliotti M., De Matteis P., “Aero-thermal Trade-off Analysis of the Italian USV Re-entry Flying Test Bed”, 14th AIAA-AHI Space Planes and Hypersonic Systems and Technologies Conference, AIAA paper 2006-8114, November 2006.
- [7] Pope R.B., “Stagnation-Point Convective Heat Transfer in Frozen Boundary Layers”, AIAA Journal, Vol. 6, No. 4, April 1968.
- [8] Chiarelli C. “Report on the CFD activities and results for Δ PDR”, AAS-I, 28 February 2006.
- [9] Hankey W. L., “Re-Entry Aerodynamics”, AIAA Education Series, J.S. Przemieniecki Series Editor-in-Chief, 1988.



This page has been purposely left blank